

See discussions, stats, and author profiles for this publication at: <https://www.researchgate.net/publication/365624968>

Drop impact dynamics on solid surfaces

Article in Applied Physics Letters · November 2022

DOI: 10.1063/5.0124256

CITATIONS
29

READS
1,236

8 authors, including:



Wei Fang

Tianjin University

33 PUBLICATIONS 631 CITATIONS

[SEE PROFILE](#)



Kaixuan Zhang

Nankai University

39 PUBLICATIONS 325 CITATIONS

[SEE PROFILE](#)



Cunjing Lv

Tsinghua University

106 PUBLICATIONS 2,613 CITATIONS

[SEE PROFILE](#)



Chao Sun

Tsinghua University

323 PUBLICATIONS 10,055 CITATIONS

[SEE PROFILE](#)

Drop impact dynamics on solid surfaces F

Cite as: Appl. Phys. Lett. 121, 210501 (2022); <https://doi.org/10.1063/5.0124256>

Submitted: 04 September 2022 • Accepted: 04 November 2022 • Published Online: 21 November 2022

 Wei Fang,  Kaixuan Zhang, Qi Jiang, et al.

COLLECTIONS

 This paper was selected as Featured



[View Online](#)



[Export Citation](#)

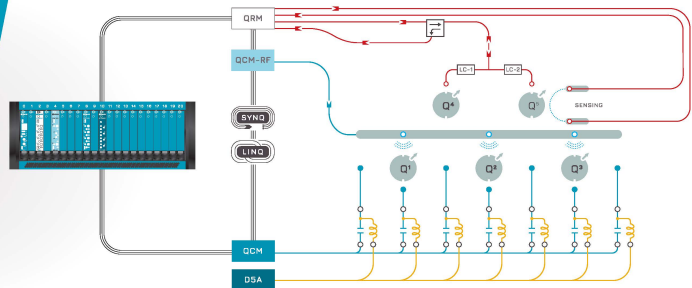


[CrossMark](#)

 QBLOX

Integrates all
Instrumentation + Software
for Control and Readout of
Spin Qubits

[visit our website >](#)



Drop impact dynamics on solid surfaces

Cite as: Appl. Phys. Lett. **121**, 210501 (2022); doi: [10.1063/5.0124256](https://doi.org/10.1063/5.0124256)

Submitted: 4 September 2022 · Accepted: 4 November 2022 ·

Published Online: 21 November 2022



View Online



Export Citation



CrossMark

Wei Fang,¹ Kaixuan Zhang,¹ Qi Jiang,¹ Cunjing Lv,¹ Chao Sun,² Qunyang Li,^{1,3} Yanlin Song,⁴ and Xi-Qiao Feng^{1,3,a)}

AFFILIATIONS

¹Institute of Biomechanics and Medical Engineering, Applied Mechanics Laboratory, Department of Engineering Mechanics, Tsinghua University, Beijing 100084, China

²Center for Combustion Energy, Key Laboratory of Thermal Science and Power Engineering of Ministry of Education, Department of Energy and Power Engineering, Tsinghua University, Beijing 100084, China

³State Key Laboratory of Tribology in Advanced Equipment, Tsinghua University, Beijing 100084, China

⁴Key Laboratory of Green Printing, Beijing National Laboratory for Molecular Sciences, Institute of Chemistry, Chinese Academy of Sciences, Beijing 100190, China

^{a)}Author to whom correspondence should be addressed: fengxq@tsinghua.edu.cn

ABSTRACT

Drop impact on solid surfaces widely occurs both in nature and engineering. In this Perspective, we review the recent advances in experimental, theoretical, and numerical investigations of drop impact dynamics on solid surfaces. The relevant theoretical models and numerical methods, such as the wetting transition models and the volume-of-fluid method, are briefly described. The influences of key factors on the drop impact dynamics, and the underlying mechanisms of forces and energies, are examined. Especially, we analyze the contact time for a drop impacting on a solid surface and discuss the effective strategies to tune the dynamic impact behavior. The design principles of functional surfaces and some typical applications are also discussed. Finally, Perspectives are given on future development of the drop impact dynamics and its potential applications in diverse engineering fields.

Published under an exclusive license by AIP Publishing. <https://doi.org/10.1063/5.0124256>

I. INTRODUCTION

Water drop impinging on solid surfaces is a widely observed phenomenon in nature, which plays an important role in various biological processes and engineering applications.^{1–10} Efficient utilization and control of water drops are crucial for the achievement of biological functions of, for example, lotus leaves,¹¹ water strider legs,¹² rose petals,¹³ spider silk,¹⁴ butterfly wings,¹⁵ and desert beetles.¹⁶ Biomaterials have evolved exquisite micro-/nano-sized surface structures comprising various chemical compositions to obtain a wide diversity of wetting-related properties^{17,18} and functions.^{19–29} The wetting properties of solid surfaces can be categorized according to their contact angles with a static water drop.¹⁸ Generally, surfaces with a contact angle less than 90° are referred to be hydrophilic; otherwise, they are hydrophobic. In particular, when the contact angle of a surface is smaller than 5°, it is called a superhydrophilic surface (SHLS). On the contrary, if the contact angle is greater than 150° and meanwhile the sliding angle is less than 10°, it is called a superhydrophobic surface (SHBS).^{30,31}

Owing to the significance of drop impact dynamics in biomechanics, surface/interface engineering, and micro-/nanometer devices

and systems, many theoretical and experimental efforts have been directed toward exploring the dynamic wetting behavior of drops on natural and biomimetic surfaces.^{32–42} These studies have led to plentiful significant applications in industries and our daily life, e.g., self-cleaning,²⁵ anti-icing,⁴³ anti-fogging,⁴⁴ anti-fouling,⁴⁵ anti-corrosion,⁴⁶ anti-bacterial,⁴⁷ heat transfer,⁸ drag reduction,⁴⁸ water condensate,⁴⁹ water harvesting,⁵⁰ oil filtration,⁵¹ liquid transport,⁵² and energy harvesting.⁵³

In this Perspective, we briefly review the state-of-the-art studies on drop impact dynamics. First, we summarize the theoretical models and numerical methods for exploring the dynamic behaviors of drops impacting on solid surfaces and discuss the key factors and physical mechanisms. Then, we analyze the contact time during the drop impact process and propose the corresponding regulation strategies. Moreover, we discuss some design principles of functional surfaces and engineering applications. Finally, some Perspectives are presented.

II. DROP-SOLID INTERACTION MODELS

The study on drop impact dynamics dated back at least one century ago. In a monograph published in 1908, Worthington⁵⁴ recorded

rich splash phenomena aroused by drop impact. Due to the ubiquity and complexity of drop-related phenomena, numerous experiments have been conducted to explore the dynamic spreading, receding, and bouncing behaviors of drops impacting on a solid surface.^{34,55} A variety of theoretical models have also been proposed,^{17,18,34} with particular emphasis on complex interactions between drops and solid surfaces.^{56–60} Some fundamental theories in this field are given below.

A. Models of wetting states and wetting transition

In 1805, Thomas Young⁶¹ derived, by considering the thermodynamic equilibrium condition at the solid–liquid–gas three-phase contact line, the liquid–solid contact angle equation

$$\cos \theta_Y = \frac{\gamma_{SG} - \gamma_{SL}}{\gamma}, \quad (1)$$

where θ_Y is called Young's contact angle, and γ_{SG} , γ_{SL} , and γ are the tensions at the solid–gas, solid–liquid, and liquid–gas interfaces, respectively.

It has been found that Eq. (1) works well for physically smooth and chemically homogeneous solid surfaces. However, experiments showed that surface roughness or microstructure, which exists in most natural and artificial materials, has a significant influence on the contact angle θ .¹⁸ Wenzel^{62,63} extended Young's equation by assuming that the liquid fills all textures on the rough surface, which is referred to as Wenzel wetting state. Thus, the contact angle is predicted by

$$\cos \theta = r \cos \theta_Y, \quad (2)$$

where r is the surface roughness, defined as the ratio of the actual surface area to the projected surface area ($r \geq 1$). Furthermore, in the case when the liquid does not fully fill the textures, which is referred to as Cassie–Baxter (CB) wetting state, Cassie and Baxter^{64,65} derived the following equation for the contact angle:

$$\cos \theta = f(\cos \theta_Y + 1) - 1, \quad (3)$$

where f is the ratio of the wet surface area to the whole projected surface area.

In addition, there are many other factors, such as dynamic impact and evaporation,^{66–68} that may affect the wetting state and even trigger the transition between the Wenzel state and the Cassie–Baxter state. For example, Lafuma *et al.*⁶⁶ showed that the CB–Wenzel transition may occur when the pressure between the drop and the SHBS exceeds a certain value. Zheng *et al.*⁵⁸ derived an expression to predict the transition pressure on superhydrophobic micropillared surfaces. The influences of hierarchical surface structures on the wetting behaviors have also been investigated in recent years.^{59,69–71} These fundamental models not only help understand the rich wetting-related phenomena in nature and engineering but also provide a guide for designing functional materials with superhydrophobic or other wetting properties.^{1,72,73}

B. Scaling laws for drop spreading and contact time on solid surfaces

A drop impacting on a SHBS with a certain velocity usually experiences the processes of spreading, receding, and bouncing. The spreading factor ξ , which denotes the ratio of the maximum spreading diameter to the initial diameter of the drop, is associated with the

Weber number ($We = \rho v^2 D / \gamma$) and the Reynolds number ($Re = \rho v D / \mu$),^{74,75} where ρ , v , D , and μ stand for the mass density, impact velocity, initial diameter, and dynamic viscosity of the drop, respectively. Considering mass conservation and assuming an inviscid liquid, the maximum spreading size of the drop is controlled by the surface tension. Balancing the Laplace pressure force with the inertial deceleration of the drop, Clanet *et al.*⁷⁶ proposed a scaling relation of $\xi \sim We^{1/4}$ for a low-viscosity drop impinging on a SHBS, which has been found to be remarkably robust in the capillary regime.

The contact time, which is the period from the moment the drop first contacts the surface to its complete detachment, is an important parameter for the applications of superhydrophobic materials. By modeling the spreading–receding behavior of the drop as a harmonic spring–mass system, Richard *et al.*^{56,57} pointed out that the contact time (t_c) is generally insensitive to the impact velocity ($0.6 \leq We \leq 74$), but related to the drop mass and surface tension of the liquid, i.e., $t_c \sim (\rho R^3 / \gamma)^{1/2}$, where R is the initial drop radius. Here, $(\rho R^3 / \gamma)^{1/2}$ is referred to as the inertial-capillary timescale.

C. Thresholds of splashing and Leidenfrost effect

When the impact velocity of a drop reaches a threshold, the drastic collision may cause breakup and splash of the drop. This process is affected by the surface roughness of the substrate and may manifest in a variety of outcomes, such as prompt splash, corona splash, crown splash, contact splash, and film splash.^{34,55,77} To quantify the critical condition, Mundo *et al.*⁷⁸ proposed a dimensionless quantity, $K = We^{1/2} Re^{1/4}$. When K reaches a critical value, the drop splash may occur. Later, Riboux *et al.*⁷⁹ improved this splashing model by taking into account the effects of the gaseous atmosphere.

A superheated surface would result in an insulating vapor layer inhibiting the physical contact between the liquid and the solid, which is referred to as the Leidenfrost effect.^{80–82} The spreading and splashing behavior of a Leidenfrost drop is markedly different from that of a drop impinging on a SHBS at room temperature.^{56,57,76} The Leidenfrost effect may lead to film splashing: drops breakup before they make contact with the surface.^{35,60} Considering the drag force of the vapor flow under the drop, Tran *et al.*³⁵ found the spreading factor can be described by a scaling relation $\xi \sim We^{3/10}$ for drop impact on superheated surfaces in the capillary regime. Furthermore, Staat *et al.*^{35,83} constructed a comprehensive phase diagram to summarize the influence of Weber number and temperature on the splashing dynamics.

III. NUMERICAL METHODS

Due to the difficulty in analytical solution of drop impact problems, various numerical methods have been developed to predict the dynamics behaviors and uncover the underlying mechanisms. Typical numerical studies consider not only the hydrodynamics and contact mechanics at the macroscale,^{57,84,85} but also the capillary effects at the microscale.^{17,86–88} A few widely adopted methods are briefly described as follows.

A. Molecular dynamics method

The classical molecular dynamics (MD) method, initiated by Alder *et al.*⁸⁹ has been widely used to study the dynamics of drops. As the validity of traditional continuum theories of capillarity, e.g., the

concepts of curvature and contact angle, has been always questioned at the nanoscale, the MD method can help provide a viable explanation of these issues.^{3,90,91} In recent years, many efforts have been put forward to reveal the microscopic mechanisms of nanodroplets impacting on solid surfaces through MD simulations.^{92–95} By combining MD and molecular kinetics, Yuan *et al.*^{96,97} reported the key role of precursor membranes in electro-elastic capillarity. Patra *et al.*^{98,99} explored how nanodroplets interact with low-dimensional materials (e.g., carbon nanotubes and graphene), and simulated a droplet-activated folding process of graphene nanostructures [Fig. 1(a)].

B. Particle dynamics method

The particle dynamics (PD) method models both solid and liquid by treating them individually as a finite number of particles. As one of the most frequently used simulation methods on the micro scales, the PD methods have evolved in a variety of forms.^{100–104} Among others, the smoothed particle hydrodynamics (SPH) method¹⁰⁰ and the dissipative particle dynamics (DPD) method¹⁰⁴ exhibit high efficiency in the study of drop impact phenomena. The SPH method is friendly to the problems involving large deformation such as high-speed collision and fluid–structure interaction.¹⁰⁵ The DPD method adopts a soft interaction potential between particles such that they can overlap with

each other during the collision. By introducing the van der Waals equation of state, Pagonabarraga *et al.*¹⁰⁶ developed a many-body DPD (mDPD) method, which can nicely simulate systems with free surfaces. The mDPD method is popular for studying wetting transition processes on diversiform microstructures^{107–109} [Fig. 1(b)]. Recently, the PD methods have been frequently adopted when investigating the thermal capillary behaviors of drop motion.¹¹⁰

C. Lattice Boltzmann method

By solving discrete Boltzmann equations, the lattice Boltzmann method (LBM) calculates the consecutive propagation and collision processes of fictitious particles within discrete lattices to obtain the microscopic properties.^{111–113} Owing to its commonality and expandability, this method has been widely used to simulate the dynamical behaviors of drops impinging on SHBSs, e.g., drop bouncing, splitting, splashing, sliding, and freezing.^{114–120} For example, Zhu *et al.*^{121,122} numerically reproduced the drop impact process on a soft substrate. Liu *et al.*^{123,124} employed this method to interpret the symmetry breaking and pancake bouncing of drops on SHBSs. With a strong capability of processing complex boundary conditions, the LBM has been utilized to investigate the problems of drops hitting curved^{119,124,125} [Fig. 1(c)], macro-textured,^{126–128} and moving substrates.^{119,129,130}

D. Volume-of-fluid method

A key issue in the simulations of drop impact dynamics is how to treat the free boundaries and liquid–solid interfaces. The volume-of-fluid (VOF) method^{75,131,132} provides a simple and efficient way to track free liquid surfaces or liquid–solid interfaces and has found extensive applications in multiphase flow problems.⁷⁵ However, the problems with discontinuous interface gradients remain intractable for the VOF method. To overcome this difficulty, Sussman^{133,134} coupled the VOF method with the level-set (LS) method^{135–137} and developed a more robust method, referred to as the coupled level-set and volume-of-fluid (CLSVOF) method. The CLSVOF method has gained much attention both in academic and industrial circles to conduct numerical studies of various drop impact phenomena.^{125,138–141} For example, it has been employed to decipher the mechanisms of wetting heterogeneity-induced behaviors of drop splitting and gyrating^{53,142,143} [Fig. 1(d)].

IV. KEY FACTORS IN DROP IMPACT DYNAMICS

The impact dynamics between a drop and a solid surface is regulated by a complex set of physical and chemical factors that are often inter-coupled and time-variant. Generally, the key components of drop impact dynamics on solid surfaces include the hydrodynamic characteristics of the drop, the geometric and chemical features of the solid surface, and the external physical stimuli, as summarized in Fig. 2.

The fluid properties of drops can be characterized by a few dimensionless parameters. The deformation and movement of a drop impacting on a solid surface are commonly dictated by the inertial force, the viscous force, and the capillary force. To distinguish the relative importance of these forces and reduce the number of the involved variables, a few dimensionless numbers are often used. They mainly include (i) the Reynolds number Re , which relates the inertia and viscosity; (ii) the Weber number We , which relates the inertia and surface

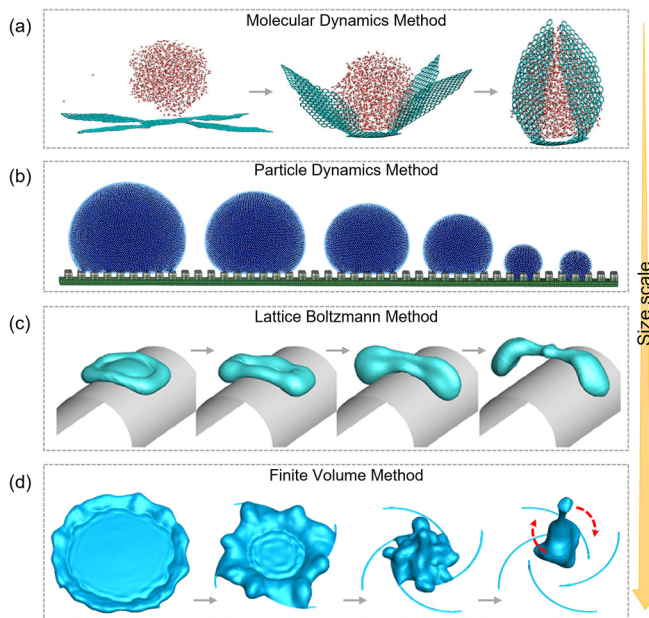


FIG. 1. Representative numerical methods of drop impact dynamics from nanoscale to macroscale. (a) Nanodroplet activates folding of graphene nanostructures simulated by the MD method. Reproduced with permission from Patra *et al.*, *Nano Lett.* **9**, 3766 (2009). Copyright 2009 American Chemical Society. (b) Wetting transition on a microstructured surface simulated by the SPH method. Reproduced with permission from Shigorina *et al.*, *Phys. Rev. E* **96**, 033115 (2017). Copyright 2017 American Physical Society. (c) Drop impacting on a cylindrical SHBS simulated by the LBM. Reproduced with permission from Yun *et al.*, *Langmuir* **36**, 14864 (2020). Copyright 2020 American Chemical Society. (d) Drop gyrating after impacting on a heterogeneous surface simulated by the CLESVOF method. Reproduced with permission from Li *et al.*, *Nat. Commun.* **10**, 950 (2019); licensed under a Creative Commons Attribution (CC BY) license.

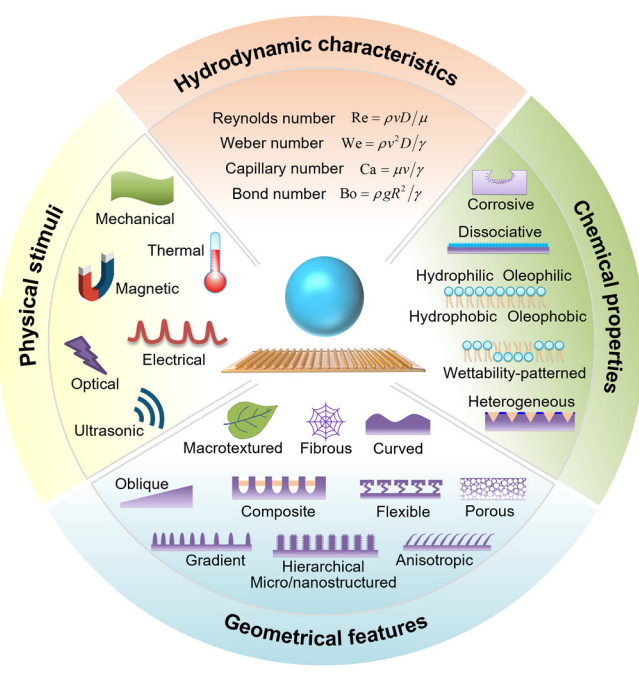


FIG. 2. Schematic illustration of key factors in the drop impact dynamics on solid surfaces. The key factors include the hydrodynamic features of the drop, the chemical and geometrical properties of the solid surface, and the external physical stimuli.

tension; (iii) the Capillary number Ca , which relates the viscosity and surface tension; and (iv) the Bond number Bo , which relates the gravity and surface tension.

In addition, the drop impact dynamics depends strongly on the chemical properties^{144,145} and geometrical features¹⁸ of the solid surface. To control the dynamic behaviors of drops, such as spreading, depositing, rebounding, and splashing, one can design solid surfaces from the following two aspects. Chemically, the wettability of a solid surface can be modified by covering the surface with organic molecules or inorganic particles. Particular reactions such as corrosion or hydrolysis of the surface may also change the solid–liquid adhesion. Geometrically, one may decorate the surface with specific macro-, micro-, or nano-sized structures. Several common forms of surface structures in textured, porous, curved, anisotropic, and other shapes are shown in Fig. 2. The presence of these structures can not only tune the hydrophilicity or hydrophobicity but also alter the boundary conditions of the flow that affect the overall motion of the drop. The surface fraction (ϕ_s) and roughness (r) are often used to characterize the topography of the solid–liquid contact area of a drop on a rough surface. Here, ϕ_s is also referred to as the pillar density, defined as the projected area fraction of the microposts ($\phi_s \leq 1$). The two parameters play an important role in predicting the apparent contact angle of drops on rough surfaces.

Moreover, physical fields can be utilized to control the dynamic behaviors of a drop impacting on a solid surface. The system may respond to external stimuli,^{146–149} such as mechanical, thermal, magnetic, electrical, optical, and ultrasonic cues, which can introduce additional energies to regulate the outcome of the system.

V. CONTACT TIME OF DROP IMPACT

Rapid removal of water drops from a solid surface is of great interest for a wide range of applications, e.g., anti-fogging, anti-icing, and self-cleaning. The contact time during the impact process of a drop on a solid surface has attracted much attention in recent years. For millimetric water drops impinging on a SHBS, the contact time is approximately independent of the impact velocity ($>0.1 \text{ m s}^{-1}$)^{56,57}

$$t_c = k \sqrt{\frac{\rho R^3}{\gamma}}, \quad (4)$$

where k is a constant coefficient determined by the surface properties. For a lotus leaf,¹⁵⁰ k is about 2.3.

Much effort has been made toward regulating the contact time by, for example, designing elaborate structures on solid surfaces (Fig. 3). By decorating a SHBS with macroscopic textures ($>100 \mu\text{m}$),^{150,151} on which the contact time has almost fallen by half compared to that on the SHBS without textures. This is due to the fact that the drop after impact tends to split on the SHBS with the textures and the splitting accelerates the recoiling speed. For a flattened drop after impact, the drop should contract symmetrically with speed¹⁵⁰

$$v_r = \sqrt{\frac{2\gamma}{\rho h}}, \quad (5)$$

where h is the thickness of the flattened drop. Since the texture makes the drop uneven in thickness, the speed would be faster in the textured regions according to Eq. (5). This regulating strategy has been demonstrated by various macroscopic textures, such as beads¹⁵² and radges.¹⁵³ Importantly, the contact time can also be reduced even when the characteristic size of the texture (i.e., curved^{124,139,140} and conical surfaces¹⁵⁴) is comparable to the drop diameter. The reduction of contact time on such surfaces results from the redistribution of the drop mass, which influences the vibrational frequency of the spring-mass system, and the viscous drag of the surrounding airflow.

To further shorten the contact time, Liu *et al.*¹²³ devised a different strategy that realizes a pancake bouncing on a solid surface. Submillimeter-scale tapered posts (diameter $\sim 100 \mu\text{m}$, and height $\sim 1 \text{ mm}$) with nanoscale superhydrophobic coatings are decorated on the surface. They found that the retracting process of the drop was eliminated and the contact time was reduced by 80% approximately. This strategy requires relatively large and tall surface structures so that the liquid can only partially penetrates the structures, without losing the Cassie–Baxter wetting state during the whole impact process.^{126,128} The penetrated Cassie–Baxter state stores an amount of capillary energy, which will convert to kinetic energy and provide the drop an upward thrust.

When the size of surface structures decreases to $\sim 100 \text{ nm}$, their topographical features may significantly alter the contact time. A recent study¹⁵⁵ showed that the contact time was reduced by about 14% on a solid surface with high solid-fraction nanoscale textures ($\sim 100 \text{ nm}$). According to the inertial–capillary timescale, the elastic impact process is dominated by the inertial force and surface tension. However, when the nanostructures are sufficiently compact ($0.25 < \phi_s < 0.64$), the line tension (the excess free energy of a three-phase contact line per unit length¹⁵⁶) produces an increasingly positive effect on the early liftoff of the drop. By incorporating the line energy, Eq. (4) can be modified as¹⁵⁵

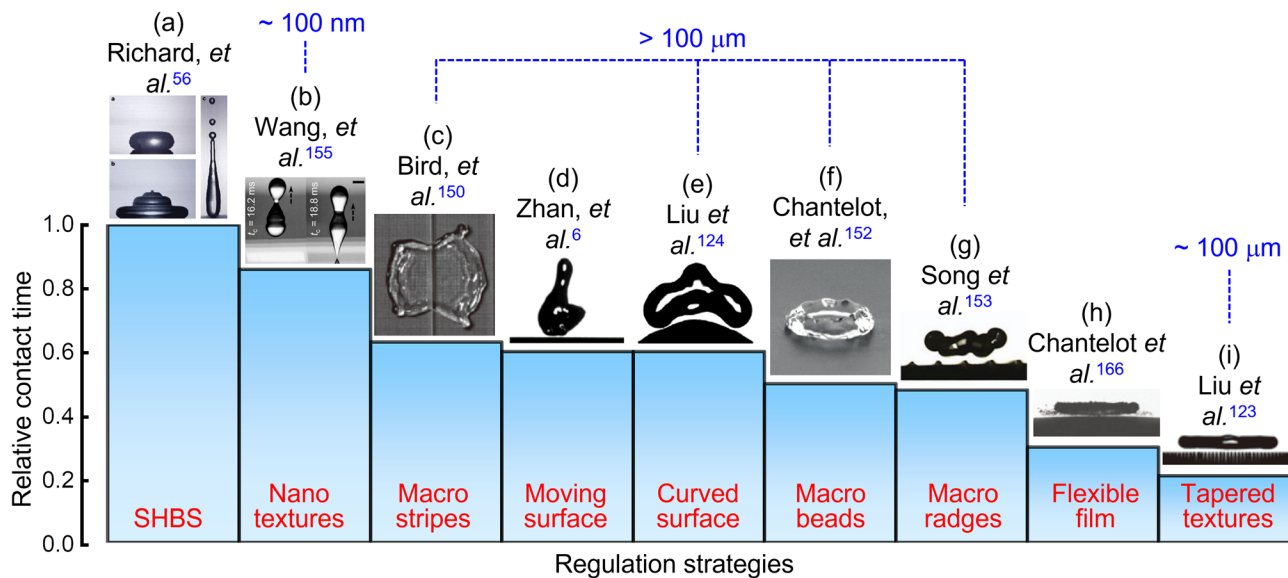


FIG. 3. Strategies for regulating the relative contact time of drops. Some typical designs of SHBSs for reducing the contact time: (a) general case. Reproduced with permission from Richard et al., *Nature* **417**, 811 (2002). Copyright 2002 Springer Nature. (b) Coated with compact nano textures. Reproduced with permission from Wang et al., *Sci. Adv.* **6**, eabb2307 (2020). Copyright 2020 Authors, licensed under a Creative Commons Attribution (CC BY) license. (c) Coated with macro-stripe. Reproduced with permission from Bird et al., *Nature* **503**, 385 (2013). Copyright 2013 Springer Nature. (d) Moving surface. Reproduced with permission from Zhan et al., *Phys. Rev. Lett.* **126**, 234503 (2021). Copyright 2021 American Physical Society. (e) Curved surface. Reproduced with permission from Liu et al., *Nat. Commun.* **6**, 10034 (2015). Copyright 2015 Authors, licensed under a Creative Commons Attribution (CC BY) license. (f) Coated with macro-bead. Reproduced with permission from Chantelot et al., *Soft Matter* **14**, 2227 (2018). Copyright 2018 Royal Society of Chemistry. (g) Coated with macro-radges. Reproduced with permission from Song et al., *NPG Asia Mater.* **9**, e415 (2017). Copyright 2017 Authors, licensed under a Creative Commons Attribution (CC BY) license. (h) Flexible film. Reproduced with permission from Chantelot et al., *Europhys. Lett.* **124**, 24003 (2018). Copyright 2018 IOP Publishing. (i) Coated with submillimeter-scale tapered posts decorated with nanotextures. Reproduced with permission from Liu et al., *Nat. Phys.* **10**, 515 (2014). Copyright 2014 Springer Nature.

$$t_c = k \sqrt{\frac{\rho R^3}{\gamma + \Lambda \tau}} \quad (6)$$

where Λ is the contact line density, and τ is the line tension which is defined as the excess free energy per unit length of a contact line of three phases.^{156,157}

Apart from introducing surface structures, some other strategies have also been proposed to regulate the contact time. For example, when a drop hits a moving SHBS, the viscous force that arises from the air layer^{158,159} between the solid and the liquid may speed up the bouncing process by affecting the shape and dynamic behavior of the drop.^{6,160–162} In addition, a flexible superhydrophobic film^{163–165} can also achieve the pancake bouncing of a drop, because the impact force excites the film to oscillate with a springboard effect of imparting a vertical momentum back to the drop.¹⁶⁴ This mechanism takes place only when the Weber number is sufficiently large. Surprisingly, the time reduction on such a flexible superhydrophobic film can be enlarged up to 70% when the drop is coated with powders¹⁶⁶ (i.e., liquid marbles¹⁶⁷).

VI. DYNAMIC MECHANISMS

Apart from the contact time, the dynamic behaviors, including the morphological evolution, impact forces, and bouncing direction of drops, are also the important issues that have received much attention.

A. Drop deposition and splitting

If the target solid surface is hydrophilic, the drop would finally adhere to the substrate, as observed in many natural and industrial processes, e.g., spaying,¹⁶⁸ inkjet printing,¹⁶⁹ and water harvesting.^{14,16} In this situation, the morphology of drop deposition is of great interest for many engineering^{26,40,170} and biomedical^{171,172} applications. On the contrary, if the substrate is hydrophobic or superhydrophobic, the drop would bounce off the solid surface after the impact. Robust control of the bouncing behavior of the drop may help design advanced surfaces with self-cleaning, anti-fogging, anti-icing, or other functions.

The achievement of efficient drop deposition on SHBS is also of significance for applications such as herbicides or pesticides on plant leaves, many of which are hydrophobic.^{168,176,177} To restrain the recoil and splash of drops on hydrophobic surfaces, one can not only design a highly adhesive surface (refer to the petal effect^{13,178}) but also provide some additives (e.g., flexible polymers¹⁷⁶ and vesicular surfactants¹⁶⁸) into the liquid. These methods can improve the deposition of drops. Therein the highly adhesive surface enlarges the pinning force along the contact line, whereas the polymers and surfactants regulate the viscosity and surface tension of the liquid, respectively [Fig. 4(a)]. Though most of these studies explored the dynamic drop behaviors at room temperature, drop deposition on high-temperature surfaces remains a puzzle, which poses a limit for the aforementioned strategies to enhance the heat transfer efficiency of solid surfaces.⁸ Due to the Leidenfrost effect, a vapor film generated from the evaporation of

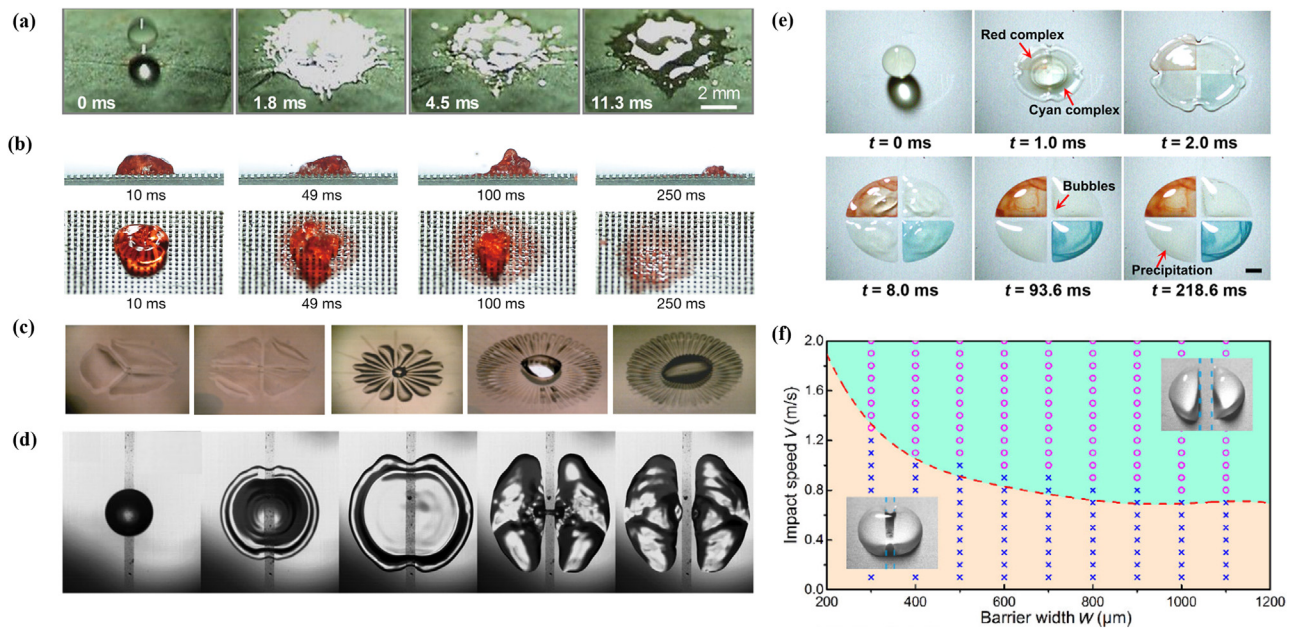


FIG. 4. Dynamics of drop deposition and splitting. (a) Controlling drop deposition on SHBSs. Reproduced with permission from Song *et al.*, *Sci. Adv.* **3**, e1602188 (2017) Copyright 2017 Authors, licensed under a Creative Commons Attribution (CC BY) license. (b) Controlling drop deposition by inhibiting the Leidenfrost effect. Reproduced with permission from Jiang *et al.*, *Nature* **601**, 568 (2022). Copyright 2022 Springer Nature. (c) Controlling drop deposition morphology on wettability-patterned surfaces. Reproduced with permission Lee *et al.*, *Phys. Fluids* **22**, 072101 (2010). Copyright 2010 AIP Publishing. (d) Controlling drop splitting on hydrophilic surfaces with superhydrophobic stripes. Reproduced with permission from Song *et al.*, *Phys. Chem. Chem. Phys.* **17**, 13800 (2015). Copyright 2015 Royal Society of Chemistry. (e) Controlling drop splitting on patterned adhesive surfaces. (f) Theoretical critical conditions for drop splitting. (e) and (f) Reproduced with permission from Li *et al.*, *Angew. Chem., Int. Ed.* **59**, 10535 (2020). Copyright 2020 John Wiley and Sons.

liquid isolates the drop from the solid surface. Jiang *et al.*⁸ designed a composite microstructural surface with underlying microchannels for vapor evacuation, which can efficiently inhibit the Leidenfrost effect and, thus, promote drop deposition [Fig. 4(b)].

Owing to the advances in material manufacture and surface modification technologies, rich surface micro-patterns can be fabricated to precisely control the drop deposition morphology, which facilitates many applications such as water collection and condensation.^{171,179} For example, a drop impacting on a hydrophilic surface with radial hydrophobic stripes will breakup and spontaneously deposit on the substrate in a multi-petaled flower shape,¹⁸⁰ as shown in Fig. 4(c). This is because the low-adhesive hydrophobic stripes could lead to splitting of the drop [Fig. 4(d)].^{181,182} Different from the conventional understanding that the splitting originates from the hydrophilicity difference, this special drop splitting originates from non-synchronous retraction of the contact line, i.e., the liquid recedes faster along the stripe than the other directions. Hence, by restraining the recoil of liquid on either side of the stripe, the drop splitting can be realized. This self-splitting behavior may also occur when the stripe is less adhesive than the sides, regardless of the hydrophilicity of the stripe or other areas [Fig. 4(e)].¹⁴² It is noteworthy that the hydrophobic or adhesive stripes should have sufficiently small sizes to accomplish the drop splitting. A recent work¹⁴² provided a theoretical model to predict the minimum width of the stripes and the scaling relation between the stripe width and the Weber number of the impacting drop, as shown in Fig. 4(f).

B. Drop impact forces

In addition to the morphological features of the impacting drops, the impact forces and stress distributions are also essential for revealing the physical essence of impact dynamics.^{39,183} To measure the temporal evolution of the drop impact force, experimental tools such as piezoelectric sensors,^{39,184} cantilever beams,^{85,185} and elastic plates^{186,187} are frequently used. As the peak force induced by the impact is one of the key parameters in the dynamic process, its magnitude is often examined. Based on the experimental results, when inertia dominates the impact process, the value of the peak force will be proportional to the square of impact velocity⁸⁵

$$F_p \sim \rho R^2 V^2, \quad (7)$$

where V is the impact velocity of the drop. On the contrary, when viscosity dominates the impact process ($\text{Re} < 20$), the dimensionless peak force, which is taken as $F_p^* \sim F_p / \rho R^2 V^2$, decreases rapidly with the Reynolds number in a power law relation.¹⁸⁸ Surprisingly, a recent work¹⁸⁹ found two local peak forces would occur during the impact process, and the second one can be even remarkably larger than the first one. This work revealed that the first local peak originated from the inertial shock between the drop and the solid, while the second local peak arose from the Worthington jet¹⁹⁰ (triggered by the singularity occurring at the collapse of an air cavity).

The impact force is the macroscopic consequence of impact pressure underneath impacting drops. However, the impact pressure is

distributed very unevenly and contains much more detailed information about the dynamics of drop impact.¹⁹¹ Due to the limitations in the temporal and spatial resolution of current measurement techniques, it is yet a huge challenge to directly measure the pressure distribution over the contact area. Theoretical or numerical methods are useful for revealing detailed information of the impact pressure. During the early stage of drop impact on a solid surface, the pressure field shows a self-similar structure where a maximum value occurs near the contact line but not at the center point of impact.¹⁹² An annular divergent form of the pressure distribution proposed by Philippi *et al.*¹⁹² is

$$p(x, t) = \frac{3}{\pi} \frac{\rho V^2 R}{\sqrt{3VRt - x^2}}, \quad (8)$$

where t is the current time and x is the distance from the impact point ($x < \sqrt{3VRt}$). During the later stage of drop impact, the pressure

maximum moves from near the contact line to the center of contact area. Some analytical formulas for the pressure distribution are also provided in recent works.^{39,193}

C. Drop bouncing and gyrating

Diversiform bouncing behaviors of drops have been observed under different conditions. For example, drop bouncing can be triggered by drop impact,^{34,37} drop coalescence,^{49,194} drop condensation,^{195,196} and mechanical and electrical fields.^{197,198} Here, we will mainly focus on the bouncing dynamics of drops impacting on a solid surface.

The bouncing movement of a drop impacting on a solid surface can be tuned by introducing regular or irregular microstructures on the substrate.³⁶ For example, anisotropic microstructures on a SHBS may cause the drop to rebound along a specific inclined direction.^{15,199,200} As shown in Fig. 5(a), on the SHBS decorated with saw-

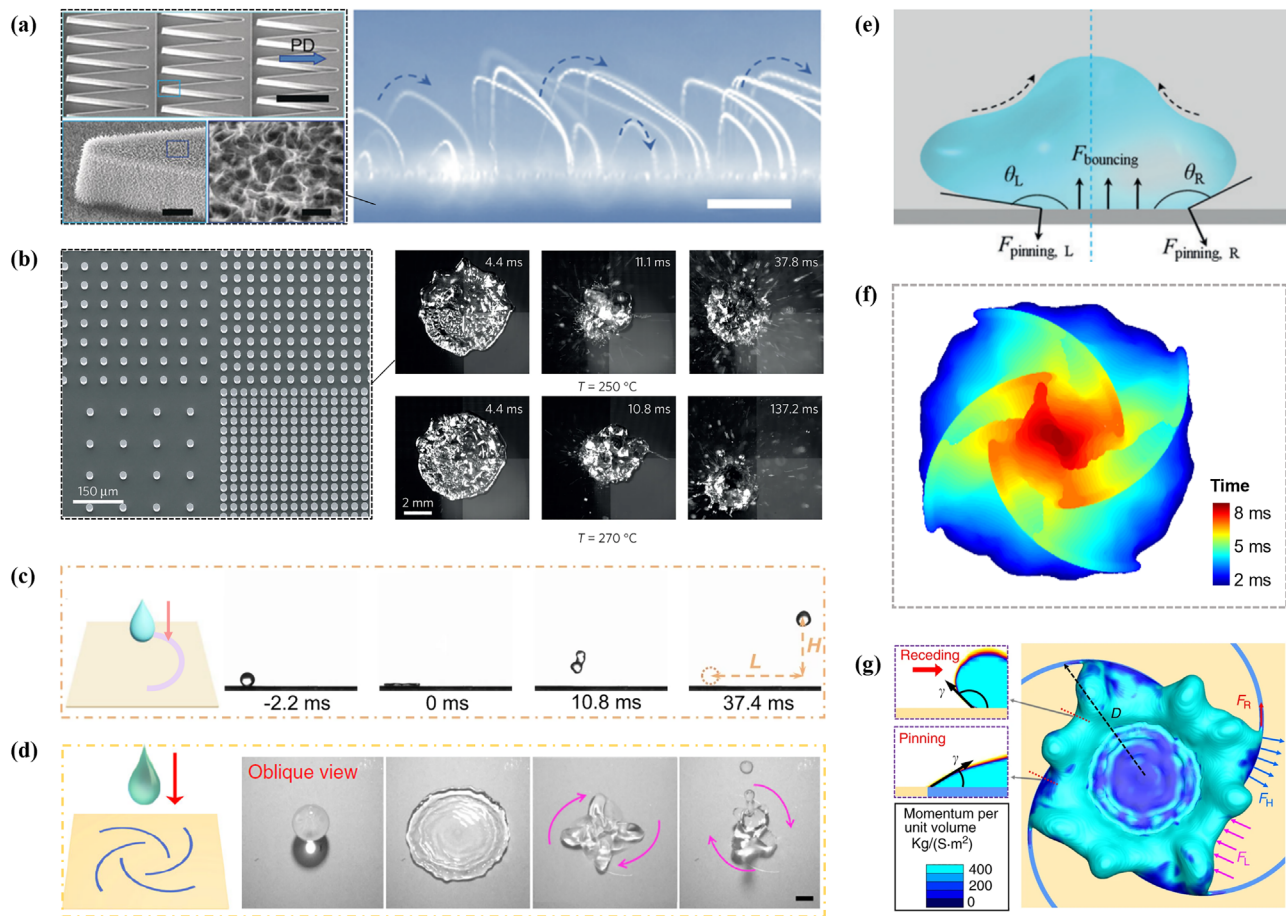


FIG. 5. Dynamics of drop bouncing and gyrating. (a) Directional bouncing of drops on the SHBS with anisotropic microstructures. (b) Directional bouncing of drops on the high-temperature microstructural surfaces. Reproduced with permission from Li *et al.*, Nat. Phys. **12**, 606 (2016). Copyright 2016 Springer Nature. (c) Directional bouncing by inhibiting drop breakage on a micro-patterned surface. Reproduced with permission from Zhao *et al.*, Nat. Commun. **12**, 6899 (2021). Copyright 2021 Authors, licensed under a Creative Commons Attribution (CC BY) license. (d) Drop gyrating on a micro-patterned surface. (e) Illustration of the asymmetric forces exerted on the retracting drop leading to preferential bouncing. (f) Contours of the solid-liquid-gas three-phase contact lines at different moments of the retraction. (g) The mechanical model to analyze the origin of the drop gyration motion. (a) and (e) Reproduced with permission from Liu *et al.*, Angew. Chem., Int. Ed. **55**, 4265 (2016). Copyright 2016 John Wiley and Sons. (d), (f), and (g) Reproduced with permission from Li *et al.*, Nat. Commun. **10**, 950 (2019). Copyright 2019 Authors, licensed under a Creative Commons Attribution (CC BY) license.

toothed micropillars, the post-impact drops could continuously jump along the parabolic paths.⁵² The direction of anisotropic microstructures fabricated by magnetic-sensitive materials can be modulated by a magnetic field such that the bouncing angle of the drop can be controlled.^{175,201} The bouncing direction depends on the net force arising from the asymmetric microstructures on the surface. As illustrated in Fig. 5(e), due to the anisotropic wettability of the surface, there is a distinct discrepancy between the contact angles at the leading edge and the trailing edge, generating an additional horizontal force on the recoiling drop.

SHBSs decorated with gradient properties can also guide the lateral bouncing of drops. The functional gradients of solid surfaces can be realized by adding spatial variations in microstructural geometries^{173,202} and/or chemical compositions.^{203,204} In addition, the gradient of surface temperature can also be utilized to affect the lateral bouncing dynamics of drops.^{10,173} As the boiling behaviors on solid surfaces are significantly affected by the surface temperature [Fig. 5(b)], the drop is subjected to an asymmetric force that influences the bouncing angle.¹⁷³

In addition to the bouncing direction of the drop, its bouncing velocity and morphology can also be influenced by the surface microarchitectures of the substrate. For example, when a drop impinges a SHBS with a hydrophilic stripe [Fig. 5(c)], its lateral momentum varies with the stripe shape (e.g., straight or curved) and the impinging position.¹⁴³ Furthermore, it was found that the stripe may significantly affect the splitting and other dynamics behaviors of the drop.¹⁴³

Interestingly, one can also maneuver the spatial movement of a drop by introducing specifically designed surface structures, which greatly influence the contact condition and the interaction forces between the drop and substrate. For illustration, Li *et al.*⁵³ found that a chiral surface architecture can drive the drop to rebound and gyrate spontaneously, as shown in Fig. 5(d). They performed numerical simulations to investigate the underlying mechanisms and demonstrated that the contact lines spread almost synchronously but recoiled at different radial velocities [Fig. 5(e)]. Based on a mechanics model, they revealed that the drop gyrating motion originated from the asymmetric pinning forces around the contact lines [Fig. 5(f)].

VII. DESIGN AND APPLICATIONS

Drop impact on solid surfaces underpins many technologically important applications. Scientists and engineers have been long interested in mimicking biological materials and reproducing their surface functions. A number of bioinspired surfaces have been designed for applications in, for example, self-cleaning,²⁵ defogging,⁴⁴ defouling,⁴⁵ heat transfer,⁸ and water condensation.⁴⁹

A. Design principles of functional surfaces

Appropriate chemical properties and microstructures are key to the design of functional surfaces. On one hand, surface wettability is often closely related to some other surface properties, such as adhesion, friction, thermal transfer, and electrical conductivity. For example, a water drop usually exchanges less heat with a superhydrophobic surface than a superhydrophilic surface during impact.²⁰⁵ The wetting property of a surface can be roughly divided into four main categories: hydrophobicity, hydrophilicity, oleophobicity, and oleophilicity.²⁰ The combination of these properties may lead to more complex performances, such as amphiphilicity and amphiphobicity. Wang *et al.*²⁷

summarized biological and biomimetic surfaces with different wetting properties and functions. It offered a useful reference for selecting materials and surface wettability in the design of surfaces with specified functions. On the other hand, to understand the relationship between microstructure geometry and surface function, Guo *et al.*²⁰⁶ classified the hierarchical surface structures of biological and biomimetic materials from a viewpoint of geometric features. They defined two indexes (m, n) to describe the constituent building elements (e.g., spheres, caves, fibers, sheets, and networks) in the hierarchical surface structures at the micro and nano scales, respectively. This classification method may offer guidance for the design of surfaces with desirable functions. It should be noted that the functions and properties of surfaces could evolve over time due to the change of surface geometry and chemistry, for example, the failure of superhydrophobicity⁷¹ or the deformation and wear of microstructure.²⁰⁷ Attention should also be paid to these factors in the design of application of these functional materials.

For the design of surfaces with complex (e.g., heterogeneous) morphological and chemical properties, it is necessary to combine theoretical or numerical methods with experiments. In addition, the machine learning method also provides a tool for multifunctional optimization of surfaces.^{208–210}

B. Applications

Controlling drop motion in three dimensions is of significance for many applications, such as water harvesting⁵⁰ and liquid transport.⁵² According to the dynamic mechanisms described in Sec. VI, a feasible way is to regulate the bouncing and rotating motions of a drop by employing a chemically or geometrically heterogeneous substrate. For example, Fig. 6(a) showed a multi-degree-of-freedom control of drop motions on wettability-patterned surfaces.⁵³ Recently, a few methods have been reported to achieve tunable wettability of surfaces by applying external stimuli, such as pressure²¹¹ and magnetic.^{201,212} As shown in Fig. 6(b), Hu *et al.*²¹¹ designed a surface coated with an array of embedded flexible chambers. By conditioning the local chamber pressure, the surface morphology could be changed, which demoed a programmable control of drop motions.

Anti-icing surfaces hold promise for critical applications in aircraft, highway, and powerline maintenance.^{43,213,214} Ice accretion occurs when water drops impact a low-temperature surface. Thereinto, the contact time and heat transfer efficiency between liquid and solid have a great influence on the process of ice formation. In addition, the pressure stability of the surface is also an important influencing factor. Considering the dynamics of drop retraction, pinning, and freezing, Mouterde *et al.*²¹⁴ presented a superhydrophobic surface with closed-cell micro-structures, which resulted in significantly enhanced effects on anti-icing than a flat hydrophilic/hydrophobic surface [Fig. 6(c)]. To avoid the CB-Wenzel transition and cushion the pressure generated by impacting drops, Wang *et al.*⁴³ designed a flexible superhydrophobic surface with hierarchical structures [Fig. 6(d)], which yielded an enhanced anti-icing ability.

Adhesion regulation of post-impact drops on biological and artificial surfaces is vital in agricultural and industrial fields. For example, an intractable problem in agriculture is to make pesticides adhere to hydrophobic leaves. To this end, Damak *et al.*⁷ proposed a surfactant-free strategy based on drop impact dynamics. They claimed that proper oil concentration and impact velocity of emulsion could greatly

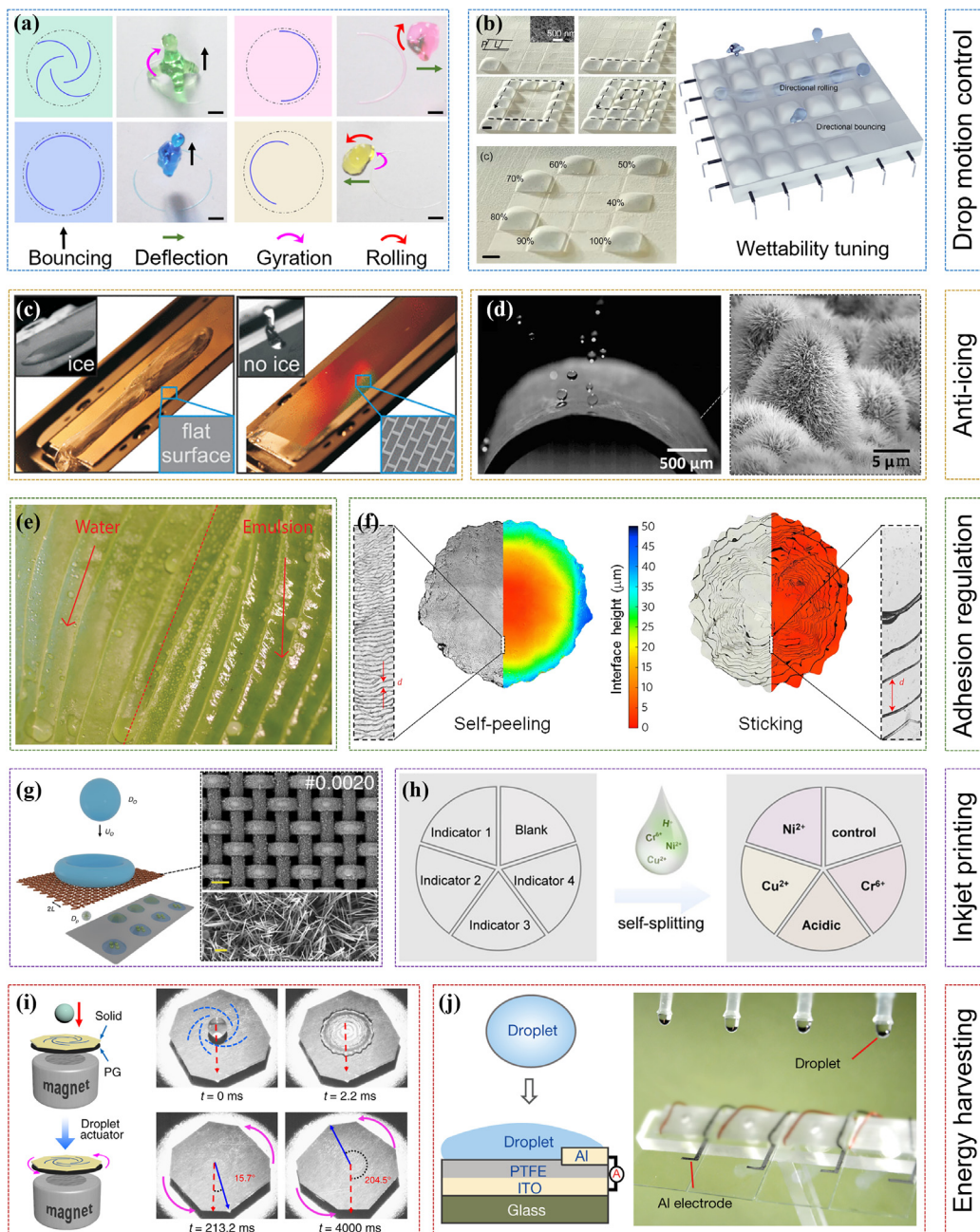


FIG. 6. Some applications of drop impact dynamics on solid surfaces. (a) and (b) Drop motion control by the wettability-patterned surface (a) and the programmable surface (b). (c) and (d) Anti-icing on the superhydrophobic surface with closed-cell micro-structures (c) and the flexible superhydrophobic surface with hierarchical structures (d). (e) and (f) Adhesion regulations of water and emulsion drops on the leave (e) and molten tin drops on the silicon wafer and glass slide (f). (g) and (h) Inkjet printing applications of drops impact on the superhydrophobic sieve (g) and the wettability-patterned surface (h). (i) and (j) Energy harvesting of the kinetic energy (i) and the electrostatic energy (j) of the impacting drops. (a) and (i) Reproduced with permission from Li *et al.*, Nat. Commun. **10**, 950 (2019). Copyright 2019 Authors, licensed under a Creative Commons Attribution (CC BY) license. (b) Reproduced with permission from Hu *et al.*, Droplet **1**, 48 (2022). Copyright 2022 Authors, licensed under a Creative Commons Attribution (CC BY) license. (c) Reproduced with permission from Mishchenko *et al.*, ACS Nano **4**, 7699 (2010). Copyright 2010 American Chemical Society. (d) Reproduced with permission from Wang *et al.*, Adv. Mater. **28**, 7729 (2016). Copyright 2016 John Wiley and Sons. (e) Reproduced with permission from Damak *et al.*, Sci. Adv. **8**, eabl7160 (2022). Copyright 2022 Authors, licensed under a Creative Commons Attribution (CC BY) license. (f) Reproduced with permission from De Ruiter *et al.*, Nat. Phys. **14**, 35 (2018). Copyright 2018 Springer Nature. (g) Reproduced with permission from Modak *et al.*, Nat. Commun. **11**, 4327 (2020). Copyright 2020 Authors, licensed under a Creative Commons Attribution (CC BY) license. (h) Reproduced with permission from Li *et al.*, Angew. Chem., Int. Ed. **59**, 10535 (2020). Copyright 2020 John Wiley and Sons. (j) Reproduced with permission from Xu *et al.*, Nature **578**, 392 (2020). Copyright 2020 Springer Nature.

improve retention of spays on hydrophobic surfaces [Fig. 6(e)]. In some other applications, impacting drops stick and solidify on the solid surface in thermal spraying. De Ruiter *et al.*²¹⁵ found that the stickiness between an impinging drop on the surface strongly depends on its impact dynamics and heat transfer with the solid. Thus, by changing the thermal conductivity, the adhesion and detachment between the drop and the surface can be regulated, as shown in Fig. 6(f).

Inkjet printing remains a leading topic in the fields of microchip printing with cells, biopolymers, and nanoparticles.⁴ To improve the printing accuracy, an ink drop is expected to be split into smaller ones. To this end, researchers attempted to adopt the satellite droplet for printing, which is generated during the drop impact or splitting process and has the advantages of low cost and small sizes.²¹⁶ As shown in Fig. 6(g), a Worthington jet would occur when a drop impacts a superhydrophobic sieve and shoot a tiny droplet through the sieve. The size of the droplet can be precisely controlled by adjusting the drop impact dynamics and the mesh size of the sieve.²¹⁷ As discussed in Sec. IV, a hydrophilic surface decorated with superhydrophobic stripes can split an impacting drop as well. This method has potential applications in biological screening and combinatorial analysis. As shown in Fig. 6(h), a micropatterned surface was used in the rapid detection of liquid drops of complex composition.¹⁴²

In addition, energy harvesting of raindrops has aroused the interest of researchers. Two kinds of energy from raindrops—kinetic energy and electrostatic energy—can be utilized. To collect the kinetic energy of the drop, Li *et al.*⁵³ established a magnetic levitation platform and decorated the surface with a chiral wettability pattern. As shown in Fig. 6(i), the heterogeneous surface constructed a minuscule rotor was driven to rotate by the reactionary torque from the impacting drop. The contact between raindrops with insulating polymer films such as polytetrafluoroethylene (PTFE) can cause triboelectricity. As the continuous impact and detachment of drops, the cycled process can be utilized for hydroelectric power generation.^{218,219} Recently, Xu *et al.*² designed a device consisting of an electrode and an indium tin oxide substrate coated with PTFE [Fig. 6(j)], largely increasing energy harvesting efficiency.

VIII. SUMMARY AND PROSPECTS

In this Perspective, we have reviewed the state-of-the-art studies of drop impact dynamics on biological and artificial solid surfaces. Particular attention has been paid to the recent experimental, theoretical, and numerical efforts for exploring the dynamic behaviors and the underlying mechanisms. The theoretical models and numerical methods have revealed the complicated physical mechanisms of rich phenomena of drop impact and bouncing from the viewpoints of energy, forces, and motions. Various surface structures of substrates at the macro, micro, and nano scales have been designed to regulate the morphologies and movements of the drops. Especially, a number of strategies have been proposed to tune the contact time during the drop–substrate impact process. These studies have not only deepened our understanding of the rich drop dynamic phenomena in nature, but also helped design functional materials for a diversity of engineering applications.

Despite the significant advances in the field of drop impact dynamics, there are still many challenges that deserve more systematic exploration. First, the drop impact behaviors are dependent on the mechanical properties of the drop itself, the geometric and mechanical

features of the substrate, the speed and direction of impact, as well as many other factors. There is still a lack of universal theoretical models and numerical methods that can predict the generic dynamic behaviors of drops, especially under extreme conditions such as very high impact speeds. Second, in engineering applications, the systems are often operated under complex physical conditions, such as electric and magnetic fields, temperature, corrosion, and surface deformation, all of which can influence the drop impact dynamic behaviors.^{144,146–149}

Further theoretical and numerical efforts, including the machine learning method, are needed to investigate the impact problems involving multiple physical fields/loads. For example, a freezing drop with evolving solidification shape on a cold surface is difficult to be modeled with the traditional simulation methods.²²⁰ Another example is a drop impinging on a solid surface with flexible microstructures,^{207,221} where the deformation of the drop and substrate is strongly coupled. In addition, multiscale or cross-scale approaches are desired to explore many wetting phenomena (e.g., the active depinning process of bacterial drops.²²²).

Finally, it is emphasized that, for the practical applications of drop impact dynamics in engineering, there are still many difficulties to overcome. For example, when a drop impacts on a wettability-patterned surface, one or more smaller droplets may be left on the solid surface, leading to mass loss of the drop.^{53,143} Optimal design of surface structures is needed to minimize the mass loss and improve the corresponding functions. The dispersal of plant seeds and spores²²³ inspires us to regulate the drop impact behaviors by invoking the elastic deformation of the substrate and even the airflow beneath the drop impact. In addition, the measurement and visualization of the interior flow inside a small drop impacting on a microstructured surface with a high speed remains a challenge, especially under some extremely severe conditions (e.g., rapidly rotating blades of aircrafts).

ACKNOWLEDGMENTS

This work was supported by the National Natural Science Foundation of China (Nos. 11921002 and 12032014) and the China Postdoctoral Science Foundation (Nos. 2021M701905 and 2021TQ0181).

AUTHOR DECLARATIONS

Conflict of Interest

The authors have no conflicts to disclose.

Author Contributions

Wei Fang: Investigation (equal); Methodology (equal); Resources (equal); Software (equal); Writing – original draft (equal); Writing – review & editing (equal). **Kaixuan Zhang:** Data curation (equal); Investigation (equal); Methodology (equal); Writing – original draft (equal). **Qi Jiang:** Data curation (equal); Investigation (equal); Writing – original draft (equal); Writing – review & editing (equal). **Cunjing Lv:** Supervision (equal); Writing – original draft (equal); Writing – review & editing (equal). **Chao Sun:** Methodology (equal); Writing – original draft (equal); Writing – review & editing (equal). **Qunyang Li:** Methodology (equal); Project administration (equal); Writing – original draft (equal); Writing – review & editing (equal). **Yanlin Song:** Project administration (equal);

Writing – original draft (equal); Writing – review & editing (equal). **Xi-Qiao Feng:** Conceptualization (equal); Funding acquisition (equal); Investigation (equal); Methodology (equal); Project administration (equal); Supervision (equal); Writing – original draft (equal); Writing – review & editing (equal).

DATA AVAILABILITY

Data sharing is not applicable to this article as no new data were created or analyzed in this study.

REFERENCES

- ¹D. Wang, Q. Sun, M. J. Hokkanen, C. Zhang, F.-Y. Lin, Q. Liu, S.-P. Zhu, T. Zhou, Q. Chang, B. He, Q. Zhou, L. Chen, Z. Wang, R. H. A. Ras, and X. Deng, *Nature* **582**, 55 (2020).
- ²W. Xu, H. Zheng, Y. Liu, X. Zhou, C. Zhang, Y. Song, X. Deng, M. Leung, Z. Yang, R. X. Xu, Z. L. Wang, X. C. Zeng, and Z. Wang, *Nature* **578**, 392 (2020).
- ³Q. Yang, P. Z. Sun, L. Fumagalli, Y. V. Stebunov, S. J. Haigh, Z. W. Zhou, I. V. Grigorieva, F. C. Wang, and A. K. Geim, *Nature* **588**, 250 (2020).
- ⁴R. K. Kumar, T. A. Meiller-Legrand, A. Alcinesio, D. Gonzalez, D. A. I. Mavridou, O. J. Meacock, W. P. J. Smith, L. Zhou, W. Kim, G. S. Pulcu, H. Bayley, and K. R. Foster, *Nat. Commun.* **12**, 857 (2021).
- ⁵S. Lyu, H. Tan, Y. Wakata, X. Yang, C. K. Law, D. Lohse, and C. Sun, *Proc. Natl. Acad. Sci. U. S. A.* **118**, e2016107118 (2021).
- ⁶H. Zhan, C. Lu, C. Liu, Z. Wang, C. Lv, and Y. Liu, *Phys. Rev. Lett.* **126**, 234503 (2021).
- ⁷M. Damak, J. De Ruiter, S. Panat, and K. Varanasi Kripa, *Sci. Adv.* **8**, eabl7160 (2022).
- ⁸M. Jiang, Y. Wang, F. Liu, H. Du, Y. Li, H. Zhang, S. To, S. Wang, C. Pan, J. Yu, D. Quéré, and Z. Wang, *Nature* **601**, 568 (2022).
- ⁹X. Li, P. Bista, A. Z. Stetten, H. Bonart, M. T. Schür, S. Hardt, F. Bodziony, H. Marschall, A. Saal, X. Deng, R. Berger, S. A. L. Weber, and H.-J. Butt, *Nat. Phys.* **18**, 713 (2022).
- ¹⁰C. Liu, C. Lu, Z. Yuan, C. Lv, and Y. Liu, *Nat. Commun.* **13**, 3141 (2022).
- ¹¹A. Marmur, *Langmuir* **20**, 3517 (2004).
- ¹²X. Gao and L. Jiang, *Nature* **432**, 36 (2004).
- ¹³L. Feng, Y. Zhang, J. Xi, Y. Zhu, N. Wang, F. Xia, and L. Jiang, *Langmuir* **24**, 4114 (2008).
- ¹⁴Y. Zheng, H. Bai, Z. Huang, X. Tian, F.-Q. Nie, Y. Zhao, J. Zhai, and L. Jiang, *Nature* **463**, 640 (2010).
- ¹⁵Y. Zheng, X. Gao, and L. Jiang, *Soft Matter* **3**, 178 (2007).
- ¹⁶A. R. Parker and C. R. Lawrence, *Nature* **414**, 33 (2001).
- ¹⁷P.-G. De Gennes, F. Brochard-Wyart, and D. Quéré, *Capillarity and Wetting Phenomena: Drops, Bubbles, Pearls, Waves* (Springer, New York, 2004).
- ¹⁸D. Quéré, *Annu. Rev. Mater. Res.* **38**, 71 (2008).
- ¹⁹T. Sun, L. Feng, X. Gao, and L. Jiang, *Acc. Chem. Res.* **38**, 644 (2005).
- ²⁰X. J. Feng and L. Jiang, *Adv. Mater.* **18**, 3063 (2006).
- ²¹X. M. Li, D. Reinhoudt, and M. Crego Calama, *Chem. Soc. Rev.* **36**, 1350 (2007).
- ²²F. Xia and L. Jiang, *Adv. Mater.* **20**, 2842 (2008).
- ²³K. Liu, X. Yao, and L. Jiang, *Chem. Soc. Rev.* **39**, 3240 (2010).
- ²⁴X. Yao, Y. Song, and L. Jiang, *Adv. Mater.* **23**, 719 (2011).
- ²⁵K. Liu and L. Jiang, *Annu. Rev. Mater. Res.* **42**, 231 (2012).
- ²⁶D. Tian, Y. Song, and L. Jiang, *Chem. Soc. Rev.* **42**, 5184 (2013).
- ²⁷S. Wang, K. Liu, X. Yao, and L. Jiang, *Chem. Rev.* **115**, 8230 (2015).
- ²⁸L. Wen, Y. Tian, and L. Jiang, *Angew. Chem., Int. Ed.* **54**, 3387 (2015).
- ²⁹M. Liu, S. Wang, and L. Jiang, *Nat. Rev. Mater.* **2**, 17036 (2017).
- ³⁰M. Ma and R. M. Hill, *Curr. Opin. Colloid Interface Sci.* **11**, 193 (2006).
- ³¹S. Wang and L. Jiang, *Adv. Mater.* **19**, 3423 (2007).
- ³²J. L. Liu and X.-Q. Feng, *Acta Mech. Sin.* **28**, 928 (2012).
- ³³L. Xu, W. W. Zhang, and S. R. Nagel, *Phys. Rev. Lett.* **94**, 184505 (2005).
- ³⁴A. L. Yarin, *Annu. Rev. Fluid Mech.* **38**, 159 (2006).
- ³⁵T. Tran, H. J. J. Staat, A. Prosperetti, C. Sun, and D. Lohse, *Phys. Rev. Lett.* **108**, 036101 (2012).
- ³⁶C. Hao, Y. Liu, X. Chen, J. Li, M. Zhang, Y. Zhao, and Z. Wang, *Small* **12**, 1825 (2016).
- ³⁷C. Josserand and S. T. Thoroddsen, *Annu. Rev. Fluid Mech.* **48**, 365 (2016).
- ³⁸G. Liang and I. Mudawar, *Int. J. Heat Mass Transfer* **106**, 103 (2017).
- ³⁹L. Gordillo, T.-P. Sun, and X. Cheng, *J. Fluid Mech.* **840**, 190 (2018).
- ⁴⁰H. Li, A. Li, Z. Zhao, L. Xue, M. Li, and Y. Song, *Acc. Mater. Res.* **2**, 230 (2021).
- ⁴¹X. Yu, Y. Zhang, R. Hu, and X. Luo, *Nano Energy* **81**, 105647 (2021).
- ⁴²X. Han, J. L. X. Tang, W. L. H. Zhao, L. Yang, and L. Wang, *Small* **18**, 2200277 (2022).
- ⁴³L. Wang, Q. Gong, S. Zhan, L. Jiang, and Y. Zheng, *Adv. Mater.* **28**, 7729 (2016).
- ⁴⁴X. Gao, X. Yan, X. Yao, L. Xu, K. Zhang, J. Zhang, B. Yang, and L. Jiang, *Adv. Mater.* **19**, 2213 (2007).
- ⁴⁵M. Kobayashi, Y. Terayama, H. Yamaguchi, M. Terada, D. Murakami, K. Ishihara, and A. Takahara, *Langmuir* **28**, 7212 (2012).
- ⁴⁶C. J. Weng, C. H. Chang, C. W. Peng, S. W. Chen, J. M. Yeh, C. L. Hsu, and Y. Wei, *Chem. Mater.* **23**, 2075 (2011).
- ⁴⁷B. Jia, Y. Mei, L. Cheng, J. Zhou, and L. Zhang, *ACS Appl. Mater. Interfaces* **4**, 2897 (2012).
- ⁴⁸G. D. Bixler and B. Bhushan, *Adv. Funct. Mater.* **23**, 4507 (2013).
- ⁴⁹J. B. Boreyko and C.-H. Chen, *Phys. Rev. Lett.* **103**, 184501 (2009).
- ⁵⁰Q. Meng, Q. Wang, H. Liu, and L. Jiang, *NPG Asia Mater.* **6**, e125 (2014).
- ⁵¹K. Li, J. Ju, Z. Xue, J. Ma, L. Feng, S. Gao, and L. Jiang, *Nat. Commun.* **4**, 2276 (2013).
- ⁵²J. Liu, H. Guo, B. Zhang, S. Qiao, M. Shao, X. Zhang, X.-Q. Feng, Q. Li, Y. Song, L. Jiang, and J. Wang, *Angew. Chem., Int. Ed.* **55**, 4265 (2016).
- ⁵³H. Li, W. Fang, Y. Li, Q. Yang, M. Li, Q. Li, X.-Q. Feng, and Y. Song, *Nat. Commun.* **10**, 950 (2019).
- ⁵⁴A. M. Worthington, *A Study of Splashes* (Longmans, Green, and Company, New York, 1908).
- ⁵⁵R. Rioboo, C. Tropea, and M. Marengo, *At. Sprays* **11**, 155 (2001).
- ⁵⁶D. Richard, C. Clanet, and D. Quéré, *Nature* **417**, 811 (2002).
- ⁵⁷K. Okumura, F. Chevy, D. Richard, D. Quéré, and C. Clanet, *Europhys. Lett.* **62**, 237 (2003).
- ⁵⁸Q.-S. Zheng, Y. Yu, and Z.-H. Zhao, *Langmuir* **21**, 12207 (2005).
- ⁵⁹X.-Q. Feng, X. Gao, Z. Wu, L. Jiang, and Q.-S. Zheng, *Langmuir* **23**, 4892 (2007).
- ⁶⁰T. Tran, H. J. J. Staat, A. Susarrey-Arce, T. C. Foertsch, A. Van Houselt, H. J. G. E. Gardeniers, A. Prosperetti, D. Lohse, and C. Sun, *Soft Matter* **9**, 3272 (2013).
- ⁶¹T. Young, *Philos. Trans. R. Soc.* **95**, 65 (1805).
- ⁶²R. N. Wenzel, *Ind. Eng. Chem.* **28**, 988 (1936).
- ⁶³R. N. Wenzel, *J. Phys. Chem.* **53**, 1466 (1949).
- ⁶⁴A. Cassie and S. Baxter, *Trans. Faraday Soc.* **40**, 546 (1944).
- ⁶⁵A. Cassie, *Discuss. Faraday Soc.* **3**, 11 (1948).
- ⁶⁶A. Lafuma and D. Quéré, *Nat. Mater.* **2**, 457 (2003).
- ⁶⁷C. Lee, Y. Nam, H. Lastakowski, J. I. Hur, S. Shin, A. L. Biance, C. Pirat, C. J. Kim, and C. Ybert, *Soft Matter* **11**, 4592 (2015).
- ⁶⁸P. Papadopoulos, L. Mammen, X. Deng, D. Vollmer, and H.-J. Butt, *Proc. Natl. Acad. Sci. U. S. A.* **110**, 3254 (2013).
- ⁶⁹X. Y. Ji, J. W. Wang, and X.-Q. Feng, *Phys. Rev. E* **85**, 021607 (2012).
- ⁷⁰H.-Y. Guo, B. Li, and X.-Q. Feng, *Nanotechnology* **28**, 384001 (2017).
- ⁷¹W. Fang, H. Y. Guo, B. Li, Q. Li, and X.-Q. Feng, *Langmuir* **34**, 3838 (2018).
- ⁷²P. Lv, Y. Xue, Y. Shi, H. Lin, and H. Duan, *Phys. Rev. Lett.* **112**, 196101 (2014).
- ⁷³Y. Li, D. Quéré, C. Lv, and Q.-S. Zheng, *Proc. Natl. Acad. Sci. U. S. A.* **114**, 3387 (2017).
- ⁷⁴B. L. Scheller and D. W. Bousfield, *AIChE J.* **41**, 1357 (1995).
- ⁷⁵M. Pasandideh Fard, Y. M. Qiao, S. Chandra, and J. Mostaghimi, *Phys. Fluids* **8**, 650 (1996).
- ⁷⁶C. Clanet, C. Béguin, D. Richard, and D. Quéré, *J. Fluid Mech.* **517**, 199 (2004).
- ⁷⁷G. E. Cossali, A. Coghe, and M. Marengo, *Exp. Fluids* **22**, 463 (1997).
- ⁷⁸C. Mundo, M. Sommerfeld, and C. Tropea, *Int. J. Multiphase Flow* **21**, 151 (1995).
- ⁷⁹G. Riboux and J. M. Gordillo, *Phys. Rev. Lett.* **113**, 189901 (2014).

- ⁸⁰G. Lagubeau, M. L. Merrer, C. Clanet, and D. Quéré, *Nat. Phys.* **7**, 395 (2011).
- ⁸¹D. Quéré, *Annu. Rev. Fluid Mech.* **45**, 197 (2013).
- ⁸²A. Bouillant, T. Mouterde, P. Bourrianne, A. Lagarde, C. Clanet, and D. Quéré, *Nat. Phys.* **14**, 1188 (2018).
- ⁸³H. J. J. Staat, T. Tran, B. Geerdink, G. Riboux, C. Sun, J. M. Gordillo, and D. Lohse, *J. Fluid Mech.* **779**, R3 (2015).
- ⁸⁴G. X. Wu, *J. Fluids Struct.* **12**, 549 (1998).
- ⁸⁵D. Soto, A. B. De Larivière, X. Boutillon, C. Clanet, and D. Quéré, *Soft Matter* **10**, 4929 (2014).
- ⁸⁶S. Ross, *J. Am. Chem. Soc.* **105**, 4871 (1983).
- ⁸⁷J. W. Van Honschoten, N. Brunets, and N. R. Tas, *Chem. Soc. Rev.* **39**, 1096 (2010).
- ⁸⁸K. Zhang, W. Fang, C. Lv, and X.-Q. Feng, *Phys. Fluids* **34**, 021302 (2022).
- ⁸⁹B. J. Alder and T. E. Wainwright, *J. Chem. Phys.* **27**, 1208 (1957).
- ⁹⁰B. Radha, A. Esfandiar, F. C. Wang, A. P. Rooney, K. Gopinadhan, A. Keerthi, A. Mishchenko, A. Janardanan, P. Blake, L. Fumagalli, M. Lozada Hidalgo, S. Garaj, S. J. Haigh, I. V. Grigorieva, H. A. Wu, and A. K. Geim, *Nature* **538**, 222 (2016).
- ⁹¹J. Fan, J. De Coninck, H. Wu, and F. Wang, *Phys. Rev. Lett.* **124**, 125502 (2020).
- ⁹²S. D. Hong, M. Y. Ha, and S. Balachandar, *J. Colloid Interface Sci.* **339**, 187 (2009).
- ⁹³T. Koishi, K. Yasuoka, S. Fujikawa, and X. C. Zeng, *ACS Nano* **5**, 6834 (2011).
- ⁹⁴F. C. Wang and Y.-P. Zhao, *Colloid Polym. Sci.* **291**, 307 (2013).
- ⁹⁵J. Koplik and R. Zhang, *Phys. Fluids* **25**, 022003 (2013).
- ⁹⁶Q. Yuan and Y.-P. Zhao, *Phys. Rev. Lett.* **104**, 246101 (2010).
- ⁹⁷Y.-P. Zhao and Q. Yuan, *Nanoscale* **7**, 2561 (2015).
- ⁹⁸N. Patra, B. Wang, and P. Král, *Nano Lett.* **9**, 3766 (2009).
- ⁹⁹J. T. Russell, B. Wang, and P. Král, *J. Phys. Chem. Lett.* **3**, 353 (2012).
- ¹⁰⁰S. Nugent and H. A. Posch, *Phys. Rev. E* **62**, 4968 (2000).
- ¹⁰¹S. Koshizuka and Y. Oka, *Nucl. Sci. Eng.* **123**, 421 (1996).
- ¹⁰²M. Zhang, *J. Comput. Phys.* **229**, 7238 (2010).
- ¹⁰³E. Shigorina, J. Kordilla, and A. M. Tartakovsky, *Phys. Rev. E* **96**, 033115 (2017).
- ¹⁰⁴P. J. Hoogerbrugge and J. M. V. A. Koelman, *Europhys. Lett.* **19**, 155 (1992).
- ¹⁰⁵X. Dong, X. Huang, and J. Liu, *Eur. J. Mech. A. Solids* **75**, 237 (2019).
- ¹⁰⁶I. Pagonabarraga and D. Frenkel, *J. Chem. Phys.* **115**, 5015 (2001).
- ¹⁰⁷J. Zhao and S. Chen, *Langmuir* **33**, 5328 (2017).
- ¹⁰⁸K. Zhang, Z. Li, M. Maxey, S. Chen, and G. E. Karniadakis, *Langmuir* **35**, 2431 (2019).
- ¹⁰⁹C. Lin, S. Chen, L. Xiao, and Y. Liu, *Langmuir* **34**, 2708 (2018).
- ¹¹⁰K. Zhang, J. Li, W. Fang, C. Lin, J. Zhao, Z. Li, Y. Liu, S. Chen, C. Lv, and X.-Q. Feng, *Phys. Fluids* **34**, 052011 (2022).
- ¹¹¹S. Chen, H. Chen, D. Martnez, and W. Matthaeus, *Phys. Rev. Lett.* **67**, 3776 (1991).
- ¹¹²Q. Zou, S. Hou, S. Chen, and G. D. Doolen, *J. Stat. Phys.* **81**, 35 (1995).
- ¹¹³S. Chen and G. D. Doolen, *Annu. Rev. Fluid Mech.* **30**, 329 (1998).
- ¹¹⁴M. Rieber and A. Frohn, *Int. J. Heat Fluid Flow* **20**, 455 (1999).
- ¹¹⁵R. J. Vrancken, H. Kusumaatmaja, K. Hermans, A. M. Preyen, O. Pierre-Louis, C. W. M. Bastiaansen, and D. J. Broer, *Langmuir* **26**, 3335 (2010).
- ¹¹⁶K. Connington and T. Lee, *J. Comput. Phys.* **250**, 601 (2013).
- ¹¹⁷R. Zhang, S. Farokhirad, T. Lee, and J. Koplik, *Phys. Fluids* **26**, 082003 (2014).
- ¹¹⁸A. Dupuis and J. M. Yeomans, *Langmuir* **21**, 2624 (2005).
- ¹¹⁹L. Fei, J. Du, K. H. Luo, S. Succi, M. Lauricella, A. Montessori, and Q. Wang, *Phys. Fluids* **31**, 042105 (2019).
- ¹²⁰J. Zhao, X. Li, and P. Cheng, *Int. Commun. Heat Mass Transfer* **87**, 175 (2017).
- ¹²¹Y. Zhu, H.-R. Liu, K. Mu, P. Gao, H. Ding, and X.-Y. Lu, *J. Fluid Mech.* **824**, R3 (2017).
- ¹²²Y. Xiong, H. Huang, and X. Y. Lu, *Phys. Rev. E* **101**, 053107 (2020).
- ¹²³Y. Liu, L. Moevius, X. Xu, T. Qian, J. M. Yeomans, and Z. Wang, *Nat. Phys.* **10**, 515 (2014).
- ¹²⁴Y. Liu, M. Andrew, J. Li, J. M. Yeomans, and Z. Wang, *Nat. Commun.* **6**, 10034 (2015).
- ¹²⁵S. Yun, *Langmuir* **36**, 14864 (2020).
- ¹²⁶L. Moevius, Y. Liu, Z. Wang, and J. M. Yeomans, *Langmuir* **30**, 13021 (2014).
- ¹²⁷A. Mazloomi M, S. S. Chikatamarla, and I. V. Karlin, *Phys. Rev. Lett.* **114**, 174502 (2015).
- ¹²⁸A. Mazloomi Moqaddam, S. S. Chikatamarla, and I. V. Karlin, *J. Fluid Mech.* **824**, 866 (2017).
- ¹²⁹S. Shen, F. Bi, and Y. Guo, *Int. J. Heat Mass Transfer* **55**, 6938 (2012).
- ¹³⁰C. Ming and L. Jing, *Comput. Math. Appl.* **67**, 307 (2014).
- ¹³¹C. W. Hirt and B. D. Nichols, *J. Comput. Phys.* **39**, 201 (1981).
- ¹³²P. R. Gunjal, V. V. Ranade, and R. V. Chaudhari, *AIChE J.* **51**, 59 (2005).
- ¹³³M. Sussman and E. G. Puckett, *J. Comput. Phys.* **162**, 301 (2000).
- ¹³⁴M. Sussman, *J. Comput. Phys.* **187**, 110 (2003).
- ¹³⁵S. Osher and J. A. Sethian, *J. Comput. Phys.* **79**, 12 (1988).
- ¹³⁶M. Sussman, P. Smereka, and S. Osher, *J. Comput. Phys.* **114**, 146 (1994).
- ¹³⁷S. H. Lee, N. Hur, and S. Kang, *J. Mech. Sci. Technol.* **25**, 2567 (2011).
- ¹³⁸Y. Shen, S. Liu, C. Zhu, J. Tao, Z. Chen, H. Tao, L. Pan, G. Wang, and T. Wang, *Appl. Phys. Lett.* **110**, 221601 (2017).
- ¹³⁹X. Liu, X. Zhang, and J. Min, *Phys. Fluids* **31**, 092102 (2019).
- ¹⁴⁰X. Liu, Y. Zhao, S. Chen, S. Shen, and X. Zhao, *Phys. Fluids* **29**, 062105 (2017).
- ¹⁴¹H. Vahabi, W. Wang, J. M. Mabry, and A. K. Kota, *Sci. Adv.* **4**, eaau3488 (2018).
- ¹⁴²H. Li, W. Fang, Z. Zhao, A. Li, Z. Li, M. Li, Q. Li, X.-Q. Feng, and Y. Song, *Angew. Chem., Int. Ed.* **59**, 10535 (2020).
- ¹⁴³Z. Zhao, H. Li, A. Li, W. Fang, Z. Cai, M. Li, X.-Q. Feng, and Y. Song, *Nat. Commun.* **12**, 6899 (2021).
- ¹⁴⁴Q. Yuan, J. Yang, Y. Sui, and Y.-P. Zhao, *Langmuir* **33**, 6464 (2017).
- ¹⁴⁵C. P. Saini, A. Barman, D. Das, B. Satpati, S. R. Bhattacharyya, D. Kanjilal, A. Ponomaryov, S. Zvyagin, and A. Kanjilal, *J. Phys. Chem. C* **121**, 278 (2017).
- ¹⁴⁶M. Abdelgawad and A. R. Wheeler, *Adv. Mater.* **21**, 920 (2009).
- ¹⁴⁷T. N. Banuprasad, T. V. Vinay, C. K. Subash, S. Varghese, S. D. George, and S. N. Varanakkottu, *ACS Appl. Mater. Interfaces* **9**, 28046 (2017).
- ¹⁴⁸D. Tian, N. Zhang, X. Zheng, G. Hou, Y. Tian, Y. Du, L. Jiang, and S. X. Dou, *ACS Nano* **10**, 6220 (2016).
- ¹⁴⁹H. Li, Y. Lai, J. Huang, Y. Tang, L. Yang, Z. Chen, K. Zhang, X. Wang, and L. P. Tan, *J. Mater. Chem. B* **3**, 342 (2015).
- ¹⁵⁰J. C. Bird, R. Dhiman, H. M. Kwon, and K. K. Varanasi, *Nature* **503**, 385 (2013).
- ¹⁵¹A. Gauthier, S. Symon, C. Clanet, and D. Quéré, *Nat. Commun.* **6**, 8001 (2015).
- ¹⁵²P. Chantelot, A. Mazloomi Moqaddam, A. Gauthier, S. S. Chikatamarla, C. Clanet, I. V. Karlin, and D. Quéré, *Soft Matter* **14**, 2227 (2018).
- ¹⁵³M. Song, Z. Liu, Y. Ma, Z. Dong, Y. Wang, and L. Jiang, *NPG Asia Mater.* **9**, e415 (2017).
- ¹⁵⁴J. Luo, F. Chu, Z. Ni, J. Zhang, and D. Wen, *Phys. Fluids* **33**, 112116 (2021).
- ¹⁵⁵L. Wang, R. Wang, J. Wang, and T.-S. Wong, *Sci. Adv.* **6**, eabb2307 (2020).
- ¹⁵⁶A. Amirfazli and A. W. Neumann, *Adv. Colloid Interface Sci.* **110**, 121 (2004).
- ¹⁵⁷S. Maheshwari, M. Van Der Hoef, and D. Lohse, *Langmuir* **32**, 316 (2016).
- ¹⁵⁸W. Bouwhuis, R. C. A. Van Der Veen, T. Tran, D. L. Keij, K. G. Winkels, I. R. Peters, D. Van Der Meer, C. Sun, J. H. Snoeijer, and D. Lohse, *Phys. Rev. Lett.* **109**, 264501 (2012).
- ¹⁵⁹R. C. A. Van Der Veen, T. Tran, D. Lohse, and C. Sun, *Phys. Rev. E* **85**, 026315 (2012).
- ¹⁶⁰H. Almohammadi and A. Amirfazli, *Soft Matter* **13**, 2040 (2017).
- ¹⁶¹X. Zhang, Z. Zhu, C. Zhang, and C. Yang, *Appl. Phys. Lett.* **117**, 151602 (2020).
- ¹⁶²S. Moghtadernejad, M. Jadidi, Z. Johnson, T. Stolpe, and J. Hanson, *Phys. Fluids* **33**, 072103 (2021).
- ¹⁶³T. Vasileiou, J. Gerber, J. Pratzsch, T. M. Schutzius, and D. Poulikakos, *Proc. Natl. Acad. Sci. U. S. A.* **113**, 13307 (2016).
- ¹⁶⁴P. B. Weisensee, J. Tian, N. Miljkovic, and W. P. King, *Sci. Rep.* **6**, 30328 (2016).
- ¹⁶⁵S. Ding, Z. Dai, G. Chen, M. Lei, Q. Song, Y. Gao, Y. Zhou, and B. Zhou, *Langmuir* **38**, 2942 (2022).
- ¹⁶⁶P. Chantelot, M. Coux, C. Clanet, and D. Quéré, *Europhys. Lett.* **124**, 24003 (2018).
- ¹⁶⁷P. Aussillous and D. Quéré, *Nature* **411**, 924 (2001).
- ¹⁶⁸M. Song, J. Ju, S. Luo, Y. Han, Z. Dong, Y. Wang, Z. Gu, L. Zhang, R. Hao, and L. Jiang, *Sci. Adv.* **3**, e1602188 (2017).

- ¹⁶⁹J. Z. Wang, Z. H. Zheng, H. W. Li, W. T. S. Huck, and H. Sirringhaus, *Nat. Mater.* **3**, 171 (2004).
- ¹⁷⁰M. Kuang, L. Wang, and Y. Song, *Adv. Mater.* **26**, 6950 (2014).
- ¹⁷¹H. Bai, L. Wang, J. Ju, R. Sun, Y. Zheng, and L. Jiang, *Adv. Mater.* **26**, 5025 (2014).
- ¹⁷²J. Chi, X. Zhang, Y. Wang, C. Shao, L. Shang, and Y. Zhao, *Mater. Horiz.* **8**, 124 (2021).
- ¹⁷³J. L. Y. Hou, Y. Liu, C. Hao, M. L. M. K. Chaudhury, S. Yao, and Z. Wang, *Nat. Phys.* **12**, 606 (2016).
- ¹⁷⁴D. Li, S. Feng, Y. Xing, S. Deng, H. Zhou, and Y. Zheng, *RSC Adv.* **7**, 35771 (2017).
- ¹⁷⁵M. Liu, C. Li, Z. Peng, S. Chen, and B. Zhang, *Langmuir* **38**, 3917 (2022).
- ¹⁷⁶V. Bergeron, D. Bonn, J. Y. Martin, and L. Vovelle, *Nature* **405**, 772 (2000).
- ¹⁷⁷M. Damak, M. N. Hyder, and K. K. Varanasi, *Nat. Commun.* **7**, 12560 (2016).
- ¹⁷⁸X. Lu, H. Cai, Y. Wu, C. Teng, C. Jiang, Y. Zhu, and L. Jiang, *Sci. Bull.* **60**, 453 (2015).
- ¹⁷⁹A. Ghosh, S. Beaini, B. J. Zhang, R. Ganguly, and C. M. Megaridis, *Langmuir* **30**, 13103 (2014).
- ¹⁸⁰M. Lee, Y. S. Chang, and H. Y. Kim, *Phys. Fluids* **22**, 072101 (2010).
- ¹⁸¹D. Song, B. Song, H. Hu, X. Du, and F. Zhou, *Phys. Chem. Chem. Phys.* **17**, 13800 (2015).
- ¹⁸²T. M. Schutzius, G. Graeber, M. Elsharkawy, J. Oreluk, and C. M. Megaridis, *Sci. Rep.* **4**(1), 7029 (2015).
- ¹⁸³X. Cheng, T.-P. Sun, and L. Gordillo, *Annu. Rev. Fluid Mech.* **54**, 57 (2022).
- ¹⁸⁴A. Sahaya Grinspan and R. Gnanamoorthy, *Colloids Surf., A* **356**, 162 (2010).
- ¹⁸⁵H. Chen, X. Zhang, B. D. Garcia, A. Georgoulas, M. Deflorin, Q. Liu, M. Marengo, Z. Xu, and A. Amirfazli, *Interfac. Phenom. Heat Transfer* **7**, 85 (2019).
- ¹⁸⁶Y. Yu and C. Hopkins, *Exp. Fluids* **59**, 84 (2018).
- ¹⁸⁷S. Mangili, C. Antonini, M. Marengo, and A. Amirfazli, *Soft Matter* **8**, 10045 (2012).
- ¹⁸⁸B. Zhang, J. Li, P. Guo, and Q. Lv, *Exp. Fluids* **58**, 125 (2017).
- ¹⁸⁹B. Zhang, V. Sanjay, S. Shi, Y. Zhao, C. Lv, X. Q. Feng, and D. Lohse, *Phys. Rev. Lett.* **129**, 104501 (2022).
- ¹⁹⁰D. Bartolo, C. Josserand, and D. Bonn, *Phys. Rev. Lett.* **96**, 124501 (2006).
- ¹⁹¹T.-P. Sun, F. Alvarez-Novo, K. Andrade, P. Gutiérrez, L. Gordillo, and X. Cheng, *Nat. Commun.* **13**, 1703 (2022).
- ¹⁹²J. Philippi, P.-Y. Lagrée, and A. Antkowiak, *J. Fluid Mech.* **795**, 96 (2016).
- ¹⁹³H. Lastakowski, F. Boyer, A. L. Biance, C. Pirat, and C. Ybert, *J. Fluid Mech.* **747**, 103 (2014).
- ¹⁹⁴J. B. Boreyko and C.-H. Chen, *Phys. Fluids* **22**, 091110 (2010).
- ¹⁹⁵T. M. Schutzius, S. Jung, T. Maitra, G. Graeber, M. Köhme, and D. Poulikakos, *Nature* **527**, 82 (2015).
- ¹⁹⁶D. Vollmer and H.-J. Butt, *Nature* **527**, 41 (2015).
- ¹⁹⁷S. J. Lee, J. Hong, K. H. Kang, I. S. Kang, and S. J. Lee, *Langmuir* **30**, 1805 (2014).
- ¹⁹⁸J. Hong and S. J. Lee, *Lab Chip* **15**, 900 (2015).
- ¹⁹⁹R. L. Agapov, J. B. Boreyko, D. P. Briggs, B. R. Srijipto, S. T. Retterer, C. P. Collier, and N. V. Lavrik, *ACS Nano* **8**, 860 (2014).
- ²⁰⁰X. Han, X. Tang, H. Zhao, W. Li, J. Li, and L. Wang, *Mater. Horiz.* **8**, 3133 (2021).
- ²⁰¹M. Cao, X. Jin, Y. Peng, C. Yu, K. Li, K. Liu, and L. Jiang, *Adv. Mater.* **29**, 1606869 (2017).
- ²⁰²S. Wang, H. Li, H. Duan, Y. Cui, H. Sun, M. Zhang, X. Zheng, M. Song, H. Li, Z. Dong, H. Ding, and L. Jiang, *J. Mater. Chem. A* **8**, 7889 (2020).
- ²⁰³Z. Zhao, H. Li, X. Hu, A. Li, Z. Cai, Z. Huang, M. Su, F. Li, M. Li, and Y. Song, *Adv. Mater. Interfaces* **6**, 1901033 (2019).
- ²⁰⁴S. Kim, M. W. Moon, and H. Y. Kim, *J. Fluid Mech.* **730**, 328 (2013).
- ²⁰⁵S. Shiri and J. C. Bird, *Proc. Natl. Acad. Sci. U. S. A.* **114**, 6930 (2017).
- ²⁰⁶H.-Y. Guo, Q. Li, H.-P. Zhao, K. Zhou, and X. Q. Feng, *RSC Adv.* **5**, 66901 (2015).
- ²⁰⁷S. Hu, X. Cao, T. Reddyhoff, D. Puhan, S.-C. Vladescu, J. Wang, X. Shi, Z. Peng, J. Demello Andrew, and D. Dini, *Sci. Adv.* **6**, eaba9721 (2020).
- ²⁰⁸Q. Wang, J. J. Dumond, J. Teo, and H. Y. Low, *ACS Appl. Mater. Interfaces* **13**, 30155 (2021).
- ²⁰⁹A. Azimi Yanchesheh, S. Hassantabar, K. Maghsoudi, S. Keshavarzi, R. Jafari, and G. Momen, *Chem. Eng. J.* **417**, 127898 (2021).
- ²¹⁰T. C. Le, M. Penna, D. A. Winkler, and I. Yarovsky, *Sci. Rep.* **9**, 265 (2019).
- ²¹¹S. Hu, X. Cao, T. Reddyhoff, X. Ding, X. Shi, D. Dini, A. J. Demello, Z. Peng, and Z. Wang, *Droplet* **1**, 48 (2022).
- ²¹²J. H. Kim, S. M. Kang, B. J. Lee, H. Ko, W.-G. Bae, K. Y. Suh, M. K. Kwak, and H. E. Jeong, *Sci. Rep.* **5**, 17843 (2015).
- ²¹³Q. Zhang, M. He, J. Chen, J. Wang, Y. Song, and L. Jiang, *Chem. Commun.* **49**, 4516 (2013).
- ²¹⁴L. Mishchenko, B. Hatton, V. Bahadur, J. A. Taylor, T. Krupenkin, and J. Aizenberg, *ACS Nano* **4**, 7699 (2010).
- ²¹⁵J. De Ruiter, D. Soto, and K. K. Varanasi, *Nat. Phys.* **14**, 35 (2018).
- ²¹⁶Y. Zhang, D. L. Y. Liu, and G. Wittstock, *Small* **14**, 1802583 (2018).
- ²¹⁷C. D. Modak, A. Kumar, A. Tripathy, and P. Sen, *Nat. Commun.* **11**, 4327 (2020).
- ²¹⁸Z.-H. Lin, G. Cheng, S. Lee, K. C. Pradel, and Z. L. Wang, *Adv. Mater.* **26**, 4690 (2014).
- ²¹⁹Z. L. D. Yang, Z. Zhang, S. Lin, B. Cao, L. Wang, Z. L. Wang, and F. Yin, *Nano Energy* **100**, 107443 (2022).
- ²²⁰S. Lyu, K. Wang, Z. Zhang, A. Pedrono, C. Sun, and D. Legendre, *J. Comput. Phys.* **432**, 110160 (2021).
- ²²¹Z. Hu, W. Fang, Q. Li, X. Q. Feng, and J. A. Lv, *Nat. Commun.* **11**, 5780 (2020).
- ²²²M. Hennes, J. Tailleur, G. Charron, and A. Daerr, *Proc. Natl. Acad. Sci. U. S. A.* **114**, 5958 (2017).
- ²²³S. Kim, H. Park, H. A. Gruszecki, D. G. Schmale, and S. Jung, *Proc. Natl. Acad. Sci. U. S. A.* **116**, 4917 (2019).